

Significance of Nonmetallic Inclusions for the Clogging Phenomenon in Continuous Casting of Steel—A Review

Susanne K. Michelic* and Christian Bernhard

Nonmetallic inclusions are well known to influence product quality and process stability in the production of steel. A process step that is very sensitive to the presence of nonmetallic inclusion (NMI) is continuous casting. Here, the so-called clogging phenomenon can occur, resulting in a distinct disruption of the casting process and decreased steel quality. The presence of nonmetallic inclusions considerably contributes to the build-up of deposits in the submerged entry nozzle provoking instabilities in the flow control system. Numerous research studies have been subject to different clogging mechanisms and related influencing parameters. Interfacial properties significantly influence the behavior of inclusions in the steel–refractory system. The present review demonstrates state of the art concerning the role of NMIs in the appearance of clogging. Particular focus is put on the wetting behavior between the different phases and their consequence for the deposition process. Industrial observations and laboratory methods are summarized and discussed; potential countermeasures are evaluated. A steel group that is especially prone to clogging are Ti–ultra low carbon (ULC) steels. An overview of the current understanding of their high clogging tendency and possible influences is presented, considering thermodynamic and interfacial aspects.

1. Introduction

Clogging is a phenomenon that usually occurs in the flow control system during the continuous casting of steel. It describes the build-up of deposits at various positions in the continuous casting machine. The submerged entry nozzle (SEN) between tundish

and mold is the area most frequently affected by the appearance of clogging.^[1–4]

The clogging problem has already occupied steelmakers and researchers for decades. One of the first studies dealing with this phenomenon was published by Snow and Shea^[5] in 1949 and Duderstadt et al.^[6] in 1968. At this time, the authors concluded that clogging is a complex problem involving the precipitation of Al₂O₃ in the nozzle. Numerous studies and publications have followed since then, dealing with possible clogging-inducing mechanisms and related countermeasures.^[7–9] The consequences of clogging are the disruption of the steel flow, which often results in an obvious quality problem of the final steel product and a necessary casting stop in the extreme case. Thus, clogging is a challenging and costly problem for the steel industry: Besides interfering with production by reducing the casting throughput and causing unscheduled nozzle exchanges, clogging is detrimental to steel cleanliness for many reasons. First, clogging

deposits that again disintegrate and are further transported in the steel flow are either trapped in the solid steel or modify the mold powder composition, leading to product defects in either case. Second, clogs change the nozzle flow pattern and jet characteristics exiting the nozzle, which disrupts the flow in the mold leading to slag entrainment and surface defects. Third, clogging interferes with the mold level control, as the flow regulating device compensates for the reduced throughput of the clogged nozzle.

In principle, the literature differentiates four main mechanisms to describe the appearance of clogging: 1) Agglomeration of deoxidation products: Nonmetallic inclusions (NMIs) from steel deoxidation and reoxidation attach to the nozzle wall by fluid flow and interfacial tension effects^[10–13]; 2) Reaction product build-up: Thermochemical reactions between the nozzle and steel lead to the (in-situ) formation of inclusions on the nozzle wall^[14–17]; 3) Oxygen diffusion: The flow of steel causes a Venturi effect region of low pressure at the inside surface of the nozzle, which draws air through the refractory resulting in inclusion formation^[18–23]; and 4) Solid steel build-up: The temperature drop because of heat transfer through the nozzle during casting decreases oxygen solubility resulting in inclusion formation at the point of lowest oxygen solubility, the steel–refractory interface.^[24–26]

In reality, a clogging deposit is often the result of more than one of the aforementioned mechanisms, which might be one of

S. K. Michelic
Christian Doppler Laboratory for Inclusion Metallurgy in Advanced Steelmaking

Montanuniversitaet Leoben
Franz Josef Straße 18, 8700 Leoben, Austria
E-mail: susanne.michellic@unileoben.ac.at

C. Bernhard
Chair of Ferrous Metallurgy
Montanuniversitaet Leoben
Franz Josef Straße 18, 8700 Leoben, Austria

 The ORCID identification number(s) for the author(s) of this article can be found under <https://doi.org/10.1002/srin.202200086>.

© 2022 The Authors. Steel Research International published by Wiley-VCH GmbH. This is an open access article under the terms of the Creative Commons Attribution License, which permits use, distribution and reproduction in any medium, provided the original work is properly cited.

DOI: 10.1002/srin.202200086

the reasons for partly contradicting results in the literature. In many studies, only one specific influencing parameter or mechanism is considered in detail. Various influencing parameters further complicate the system and the provision of proper countermeasures in a particular case. To categorize the different possibilities, metallurgical factors (e.g., deoxidation practice, ladle treatment, and tundish metallurgy) which decide the inclusion evolution must be considered.^[27–32] Moreover, refractory (e.g., porosity, wettability, chemical stability of the SEN)^[33,34] and hydrodynamic factors,^[35–38] including, for example, the fluid flow characteristics and SEN geometry, are essential. Moreover, different mechanisms are reported for the transport of inclusions to the nozzle wall: turbulent flow, turbulent recirculation zones, rough nozzle walls, and external corners. A comprehensive experimental and mathematical study on the effect of fluid flow characteristics on nozzle blockage in aluminum-killed steels has been done by Wilson et al.^[37] They addressed centripetal forces and turbulence to be responsible for the transport of Al_2O_3 particles to the nozzle wall, where they subsequently adhere. The authors also indicated that once the deposition is initiated, advancing deposition is expected due to local changes in the fluid flow behavior. It is also finally pointed out that the most effective way of reducing nozzle clogging is by reducing the amount of Al_2O_3 inclusions in the melt. A significant contribution in understanding the fluid flow in continuous casting has been done by B.G. Thomas and L. Zhang^[39] by summarizing the effects of fluid flow phenomena in the mold region and also indicating the resulting implications for process optimization. Their investigations examine the role of bubble and inclusion transport, multi-phase flow, turbulent flow in nozzle and mold as well as the factors heat transfer, electromagnetic forces, and interfacial reactions.^[7,40–43]

A systematic and comprehensive review focusing on the behavior of NMI under a swirl flow in SEN and mold has been published recently.^[44] One of the latest activities in terms of numerical simulation related to clogging has been published by H. Barati et al.^[45] who developed a transient model considering two-way coupling between clog growth (due to particle deposition) and fluid flow in the SEN. The authors describe clogging as a stochastic and self-accelerating process by considering the initial coverage of the nozzle wall with deposited particles, the evolution of a bulged clog front, and the subsequent formation of a branched structure. Recently, the same research group applied the described model also on particle deposition in Ti-stabilized ultra-low carbon (ULC) steels; a steel type that shows a high tendency toward clogging.^[46] Hydrodynamic factors and the vast number of numerical simulations performed on this phenomenon are not further considered in detail in this review. Conversely, the authors explicitly express that this limitation does not imply minor importance of the numerical work but simply is out of the focus of the present review.

Considering all the possible sources of NMIs, it can be concluded that the mechanisms of agglomeration of deoxidation products and reaction product build-up are most decisive, at least for oxide clogging. In addition to oxide clogging, clogging can also occur in other forms, depending on the steel composition and processing. An example are nitrides^[47,48] and sulfides,^[49–51] which can also provoke clogging in the SEN. In contrast to oxides and nitrides, where secondary metallurgical treatment can

essentially contribute to reduced clogging, mainly temperature control is essential for sulfide clogging.

Bernhard et al.^[52] ranked the described mechanisms based on their importance in literature and summarized the main related influencing parameters. The amount of solid oxide inclusions, respectively, the steel cleanliness level entering the SEN was found to be decisive for the clogging behavior. Despite many fundamental and applied research studies on nozzle clogging, the problem and its detailed understanding are still subject to discussion. For this reason, the review focuses on the behavior of non-metallic particles originating from steel deoxidation in secondary metallurgy and their consequence for the appearance of clogging. Metallurgical aspects, especially the role of wetting and interfacial conditions in the system steel–refractory are in the foreground of this work. Special attention is given to the group of Ti-stabilized ULC and interstitial free (IF) steels, particularly used for deep drawing applications in the automotive industry. Their increased clogging tendency is primarily a result of inclusion evolution in secondary metallurgy caused by the addition of Ti. Typically, ULC steels with and without titanium addition do not get a calcium treatment due to the process conditions in secondary metallurgy, which makes them additionally interesting to consider in the present study.

2. Inclusion-Related Parameters Influencing the Clogging Tendency in the SEN

The presence of NMIs essentially contributes to the appearance of clogging in the continuous casting process. Knowledge about their formation and modification is a key to possibly avoiding their deposition at the refractory wall during casting. Various reactions and interactions can occur during secondary metallurgy in the mentioned system. As well known, inclusions are supposed to collide and agglomerate in the liquid steel resulting in the formation of larger particles. If the inclusions are large enough, they are transported to the steel/slag interface by floatation, bubble attachment, or fluid transport. They can be removed by passing the steel/slag interface and by subsequent dissolution in the slag. Microscopic inclusions are especially prone to be transported and adhere to steel/refractory interface. Others might stay in the melt and pass on to the next process step. An aspect that is decisive for the inclusion behavior is the interfacial tension between the different participating phases, also involving the specific properties of the NMIs.^[53,54] The impact of selected inclusion properties on the clogging tendency is described in the following.

2.1. Size, Number, and Chemical Composition of Inclusions

The overall number of particularly solid NMI is a significant factor. Under the assumption, that mass build-ups in the SEN arise during casting due to the deposition of particles, an increased number of inclusions and consequently a lower steel cleanliness results in a higher growth rate of the clog. Evidence of a directly proportional relationship between the amount of Al_2O_3 inclusions in the melt and the clogging rate was, for example, described by Anderson and Wijk.^[25] The size and shape of NMIs influence, among other things, the drag force during the

floatation of a particle. Particles with a more extensive projected area toward the flow direction face an increased drag force. The particle radius governs the geometrical conditions in case of particle attraction to other NMIs, gas bubbles, and refractory walls.

The aggregate condition of a NMI at steelmaking temperatures is fixed by its chemical composition. Usually, inclusions that are liquid at casting temperatures do not cause clogging problems. This is also the explanation behind one of the probably most well-known countermeasures against clogging of solid Al_2O_3 inclusions: Ca-treatment. The addition of Ca affects the modification of solid inclusions to liquid calcium aluminates, which have a decreased tendency to adhere to the nozzle wall. The favorable region of modified liquid inclusions is often referred to as the “liquid window of castability.”^[55] Numerous studies on inclusion modification through Ca-treatment exist, investigating the effect of the added Ca-amount for different steel compositions^[55–66]. While too-low Ca-addition results in incomplete modification of existing Al_2O_3 or spinel, an excessive Ca-addition can provoke the formation of CaS in case sufficient sulfur is present. In the following, some practical examples are discussed exemplarily to illustrate changes in inclusion morphology and composition through Ca-treatment in more detail. **Figures 1** and **2** give some examples of scanning electron microscope (SEM) images and corresponding energy dispersive spectroscopy (EDS) data for different Ca/Al ratios in bearing steel. In this experimental study,^[63] the total oxygen content could be significantly reduced by complex Al–Ca deoxidation. A change in inclusion composition was observed with increasing the mass ratio of Ca/Al from 0.8–1.6 to 2.4–3.2. Inclusions were modified following the path $\text{Al}_2\text{O}_3 \rightarrow \text{CaO} \cdot 0.6\text{Al}_2\text{O}_3 \rightarrow \text{CaO} \cdot 2\text{Al}_2\text{O}_3 \rightarrow 12\text{CaO} \cdot 7\text{Al}_2\text{O}_3$, which is also in agreement with thermodynamic calculations. Cluster inclusions were found to change toward single irregular particles, which were finally assisting to form the desired low-melting-point liquid calcium aluminates. Next to the total oxygen and Ca/Al ratio, also the content of sulfur is essential. Calcium aluminates might act as a nucleation site for sulfide precipitation during solidification. CaS formation at a transient stage needs also to be considered. As an example, **Figure 3** demonstrates the modification route of an Al_2O_3 cluster through Ca-treatment for in melts with a sulfur content between 40 and 100 ppm.^[66] The shown images have been obtained by means of etching or complete dissolution of the steel matrix with a bromine methanol solution. In this case, CaS was observed as an intermediate reaction product formed immediately after Ca

addition adhering to unmodified Al_2O_3 particles. With increasing time, a change in inclusion morphology toward spherical calcium aluminates has been observed. The authors of the described work conclude that the inclusions modification by calcium in low sulfur heats (7 ppm) is significantly better as compared to high sulfur heats (100 ppm). In the medium range, between 40 and 100 ppm sulfur, no specific difference in the modification of Al_2O_3 has been observed.

Liu et al.^[62] also studied the inclusion modification through Ca-treatment in plant trials analyzing the influence of different Ca/O ratios as well as higher dissolved Al and S contents in the melt. The work also focused on validating thermodynamic calculations of the “liquid window” for these steel compositions. **Figure 4** illustrates an example for inclusion modification in the system Ca–Mg–Al–S. Inclusion compositions before and after Ca-treatment considering different Ca/O ratios are compared. The symbol size in **Figure 4** is proportional to the number fraction of inclusions of the indicated composition; the area inside the dashed line defines inclusion compositions in which the fraction of liquid should be at least 0.5 at 1823 K. It is obvious that the Ca content in the inclusions significantly increased after Ca addition; the percentage of CaS also expanded. In principle, a good agreement between experimental data and equilibrium calculations has been found.

Another study on the inclusion evolution in Ti-bearing steel with Ca-treatment has been published by Li et al.^[67] Also here, a significant difference in inclusion composition, size, and morphology before and after the addition of Ca was demonstrated. **Figure 5** illustrates inclusion evolution in the ternary system $\text{CaO}–\text{Al}_2\text{O}_3–\text{Ti}_2\text{O}_3$ for three different laboratory-scale melts with different mass fractions of Ca and Al. As shown in **Figure 5**, inclusions are mainly spherical titanium aluminates before Ca addition and there is no significant change of morphology after Ca-treatment (40 ppm Al, 5 ppm Ca). In contrast, a significant amount of irregular inclusions in the system Ca–Al–Ti–O is formed in Melt No.2 (50 ppm Al) as a result of the increased Ca content of 40 ppm. The inclusions are mostly located in the perovskite and $(\text{CaO})_3 \cdot (\text{TiO}_x)_2$ region. For Melt No.3 (400 ppm Al), almost no liquid inclusions were found before Ca-treatment also resulting in an irregular appearance. However, after Ca-treatment (25 ppm Ca), inclusions evolved to liquid calcium aluminates.

Finally, a parameter also governed by the composition of the particle is its density. The buoyancy force changes depending on

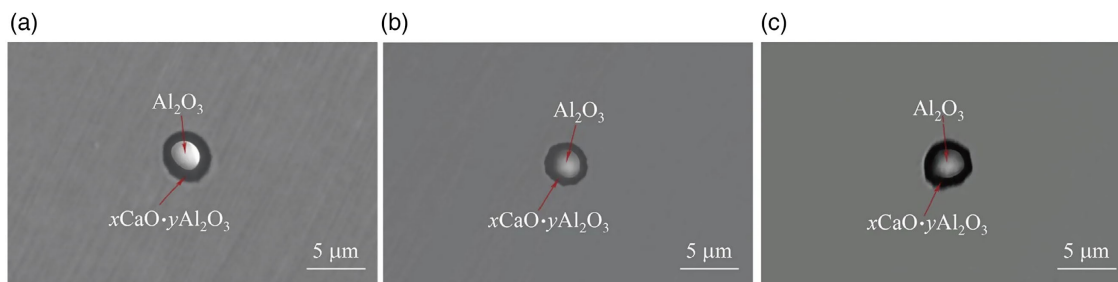


Figure 1. SEM images of three examples for complex phase inclusions (Al_2O_3 as the core of calcium aluminate) with Ca/Al ratio of 1.6. Reproduced with permission.^[63] Copyright 2019, Springer Nature.

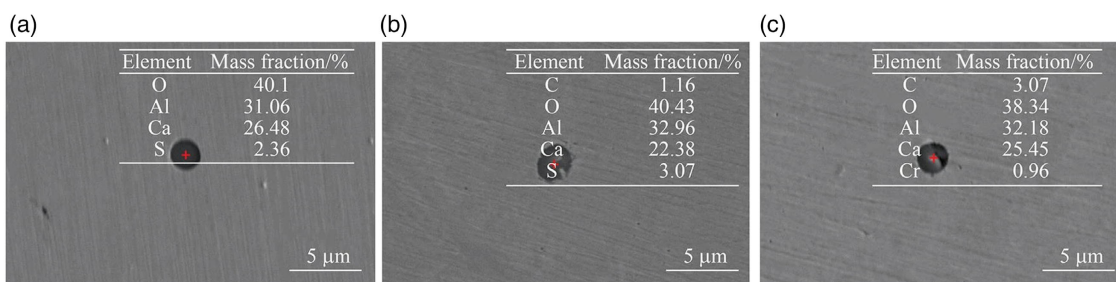


Figure 2. SEM images of three examples for liquid calcium aluminates with a Ca/Al ratio of 3.2. Reproduced with permission.^[63] Copyright 2019, Springer Nature.

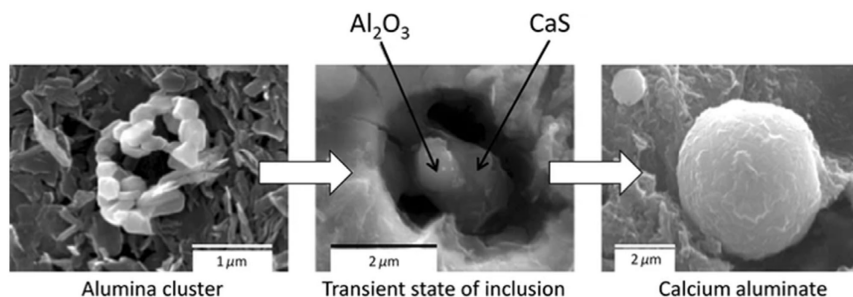


Figure 3. 3D insight into the modification route of Al_2O_3 inclusions by Ca-treatment obtained by exposing the inclusions to bromine-methanol solution. Reproduced with permission.^[66] Copyright 2011, Springer Nature.

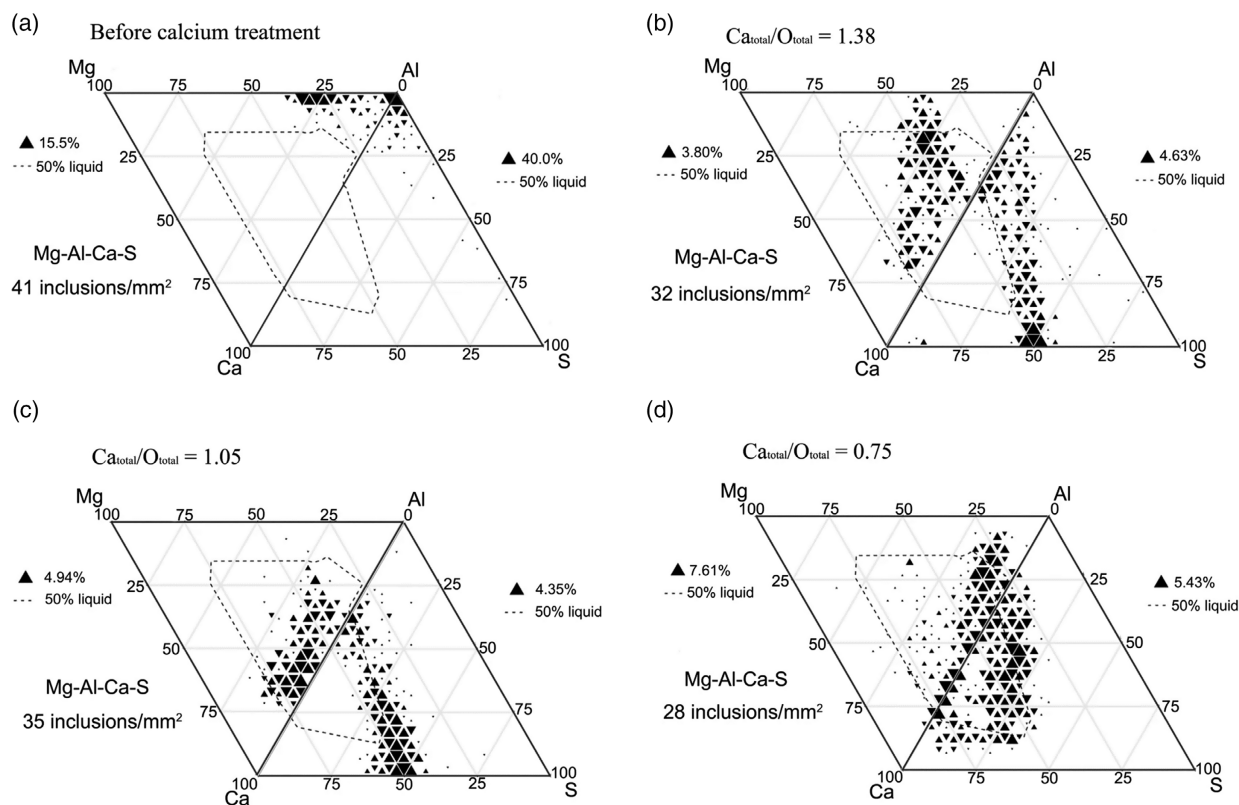


Figure 4. Inclusion compositions within the system Ca–Al–Mg–S (plotted as mole fractions): a) before Ca-treatment and b–d) after Ca-treatment considering different Ca/O ratios. Reproduced with permission.^[62] Copyright 2021, Springer Nature.

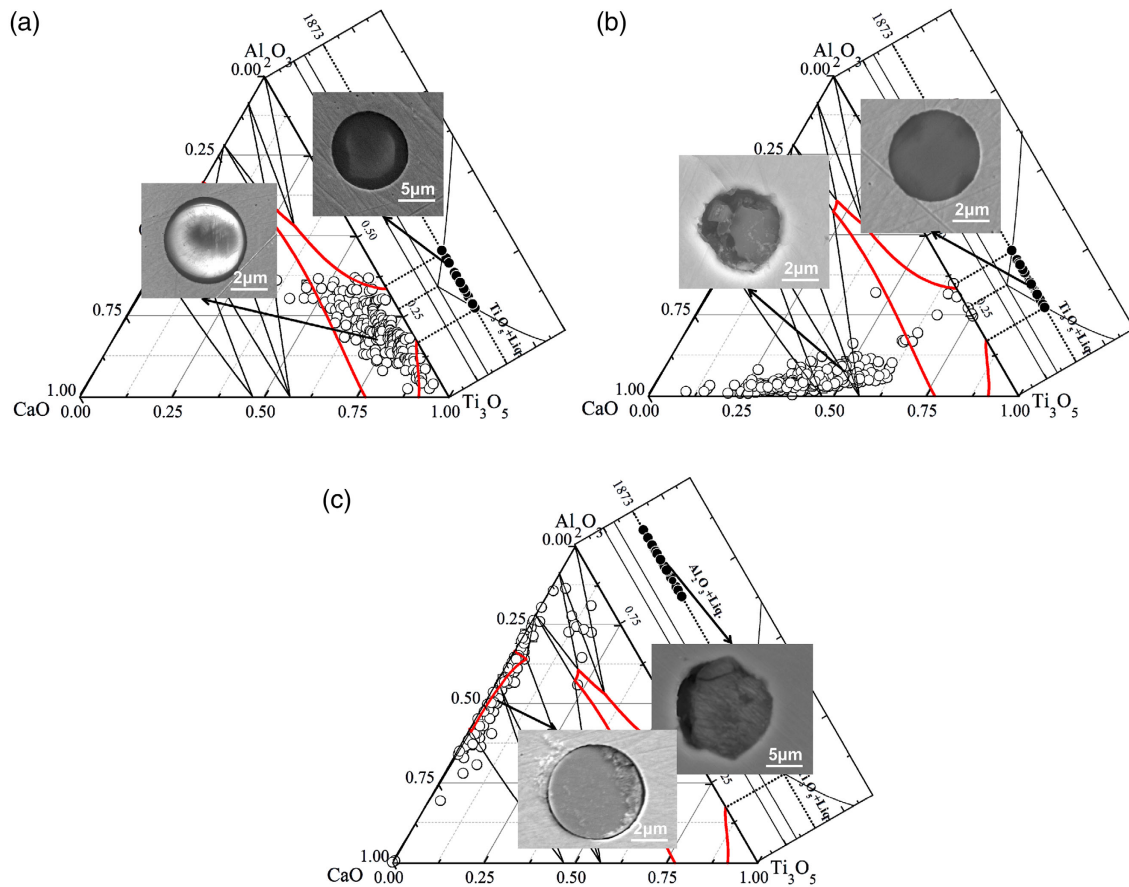


Figure 5. Inclusion compositions and morphologies in three laboratory-scale melts in the isothermal sections: a) Melt No. 1, b) Melt No. 2, and c) Melt No. 3. Thick red lines indicate the liquidus region at 1873 K. The black dots represent the specific sample before Ca, and the white ones represent the sample after Ca addition. Reproduced under the terms of the CC-BY license.^[67] Copyright 2019, The Authors, published by MDPI.

the particle density, which is again responsible for particle flotation. The lower the density of the particle, the higher the vertical velocity of the particle.

2.2. Wetting Conditions in the System Steel-Inclusion-Refractory

The contact angle between liquid steel and NMI is decisive for the inclusion behavior at the interface. A lower contact angle between the inclusion and the liquid steel, implying a better wettability of a particle, results in a decreased driving force for particle agglomeration and separation. Vice versa, a high contact angle (and insufficient wettability) supports separation and particle deposition at the refractory wall. The change in free energy ΔG in case an inclusion adheres to the refractory or a second NMI is described in **Equation (1)**,^[68] where γ_M is the surface tension of the liquid steel, θ_{I-M} is the contact angle between the inclusion and the metal, and $\cos \theta_{M-R}$ the contact angle between the metal and the refractory.

A wetting angle above 90° results in a negative free enthalpy with its minimum at a contact angle of 180° .^[54]

$$\Delta G_{I-R} = \gamma_M (\cos \theta_{I-M} + \cos \theta_{M-R}) \quad (1)$$

Figure 6 gives a schematic overview of possible wetting conditions between liquid steel and refractory/inclusions, as well as two examples of measurement results obtained from high-temperature drop shape analysis (HT-DSA). In both cases, the measured contact angle corresponds with partial non-wetting. However, the measured contact angles differ from $98^\circ \pm 5.7$ between molten steel and Al_2O_3 to $137^\circ \pm 9$ between molten steel and MgO ,^[69] which already illustrates the potential consequences on inclusion behavior as a function of inclusion type or used refractory material. A literature summary of contact angles between liquid iron/steel and various nonmetallic phases is presented in **Table 1**. Especially alumina shows comparatively high contact angles leading to a high driving force towards inclusion separation. In the case of solid calcium aluminates, a significant but weaker tendency toward separation can be concluded. Liquid inclusions such as highly modified calcium aluminates can hardly be removed from the melt as the liquid steel commonly wets them.^[70]

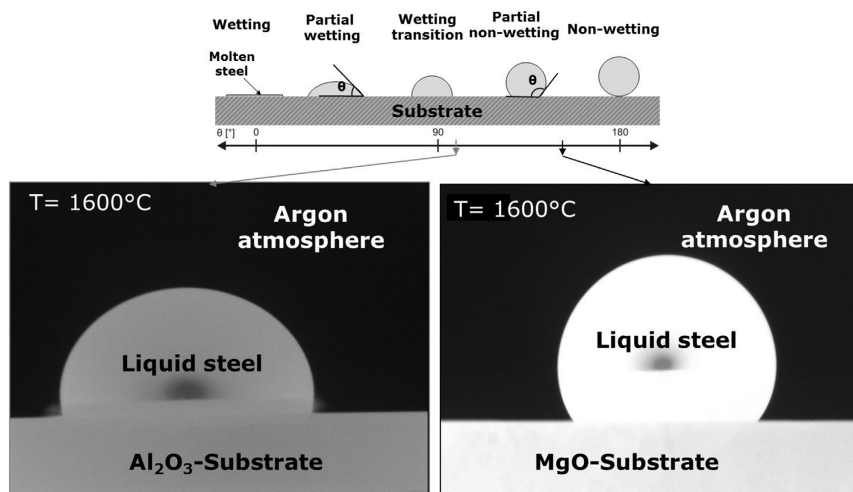


Figure 6. Schematic illustration of possible wetting conditions between liquid steel and refractory/inclusion. Reproduced with permission.^[69] Copyright 2018, Springer Nature.

3. Inclusion Deposition at the Steel/Refractory Interface

A basic understanding of the physical processes of particle deposition in the SEN is necessary to assess the clogging tendency of the inclusion population, which is created during secondary refining and on the liquid steel's path to the SEN. Following the findings of Rackers,^[71] around 16% of the particles, which enter the SEN, will get deposited. As a consequence, a higher cleanliness will decrease the overall clogging tendency. Based on an overview of SEN clogging deposits from industrial trials, experimental methods to study the clogging tendency of defined inclusions are presented and summarized. A theoretical approach for the deposition process and possible countermeasures to possibly avoid the appearance of clogging are discussed.

3.1. Characterization of Clogging Deposits from Industry

Numerous studies on the investigation of clogging deposits are available in the literature. Since clogging can appear in many different aspects depending on the specific steel grade, the processing route, and alloying, lining, and slag concepts, various phases are reported as part of the clog. For example, **Figure 7** shows two images and a corresponding X-ray diffraction (XRD) spectrum at the end of casting a P-containing high strength IF steel. The clogging layer is clearly visible at the inner wall of the SEN. Al₂O₃ was identified as the primary compound of the clog, also including small amounts of TiO₂. The ZrO₂ comes from the nozzle material.^[72] This work concluded that the P-containing high strength IF steel showed more clogging at the inner nozzle wall and a cleaner inner nozzle wall after casting than a common IF steel. Li et al.^[72] explained this due to the presence of phosphorus in the molten steel, which increases the wettability between Al₂O₃ inclusions and the refractory material.

Table 2 summarizes clog analyses results following the first described clogging mechanisms for a range of steel grades,

indicating if Ca-treatment has been performed in the specific case. Although Ca-addition is a common countermeasure to avoid clogging in Al-killed steels, several studies reported that an improper Ca-treatment might also increase clogging tendency. Especially CaO.6Al₂O₃ inclusions should definitely be avoided.^[56] Vermeulen et al.^[73] investigated the clogging behavior of non-Ca-treated steels. They determined that Al-killed steels with high manganese and high carbon content are significantly less prone to clogging than steels with low manganese and low carbon contents. A group of steels strongly affected by clogging, are Ti-stabilized ULC and IF steels.^[74–76] These steels have been and are still in the focus of research and will also be addressed in more detail in this review at a later stage.

3.2. Experimental Methods to Analyze the Inclusion Behavior in the System Steel-Refractory

In contrast to direct investigations of clogged material as shown in Section 3.1., also various laboratory methods are used to study the inclusion behavior under different conditions. Usually, isolated effects like inclusion modification or agglomeration in the liquid steel or the wettability in the system steel-inclusion-refractory are analyzed. **Table 3** summarizes potential experimental methods that have already been applied to study the behavior of NMIs and their consequence for clogging. One possibility of following the inclusion behavior is to systematically simulate the deoxidation process and the related inclusion formation and modification in laboratory experiments.^[77–80] For example, Matsuura et al.^[78] created a specific inclusion population in the melt to study the transient stages of inclusion evolution during Al and or Al/Ti additions. Through continuous sampling at different time steps with subsequent inclusion characterization by SEM/EDS measurements, the change in inclusion composition over time was studied, providing important insights for the clogging of Ti-ULC steels. Although real process conditions cannot be reproduced in most cases, e.g., considering

Table 1. Summary of contact angle values of liquid iron/steel on various nonmetallic phases.

Nonmetallic phase	Type of liquid	Temp. [°C]	Atmosphere	Contact angle θ [°]	References
Al ₂ O ₃ (s)	Fe, pure	1600	Ar	135–144	[121]
Al ₂ O ₃ (s)	Fe, Armco	1600	Ar	132–140	[82]
Al ₂ O ₃ (s)	Fe, Armco	1550	Ar/Vac	140/141	[122]
Al ₂ O ₃ (s)	Fe, pure	1550	Ar (5% H ₂)	126.9	[123]
SiO ₂ (s)	Fe, pure	1600	Ar/N ₂	112/115	[124]
CaO (s)	Fe, pure	1600	Ar	132	[125]
TiO ₂ (s)	Fe, Armco	1550	Vac	72	[122]
TiO ₂ (s)	Fe, Armco	1550	H ₂	84	[122]
Ti ₂ O ₃ (s)	Fe, pure	1550	Ar	121	[83]
MgO (s)	Fe, pure	1600	Ar	125	[121]
MgO (s)	Fe, pure	1550	Ar	130.9	[126]
MgO (s)	Fe, pure	1550	Ar (5% H ₂)	133.5	[123]
MgO·Al ₂ O ₃ (s)	Fe, pure	1550	Ar (5% H ₂)	113.7	[123]
CaS (s)	Fe, Armco	1530	Ar	87	[127]
CaO·Al ₂ O ₃ (s)	Fe-2% [C]	1500	Ar	114	[128]
CaO·2Al ₂ O ₃ (s)	Fe-2% [C]	1550	Ar	112	[128]
CaO·6Al ₂ O ₃ (s)	Fe-2% [C]	1550	Ar	123	[128]
Forsterite MgO–SiO ₂ (s) 57.6/42.4	Fe, pure	1550	Ar	82	[129]
Mullite Al ₂ O ₃ –SiO ₂ (s) 72/28	Fe, pure	1550	Ar	54	[129]
Spinel MgO–Al ₂ O ₃ (s) 28.4/71.6	Fe, pure	1550	Ar	93	[129]
Quasi-corundum MgO–Al ₂ O ₃ –SiO ₂ (s) 10/65/25	Fe, pure	1550	Ar	85	[129]
MgO–Al ₂ O ₃ –TiO ₂ (s) 50.2/0/49.8	Fe, pure	1550	Ar	127.0	[126]
MgO–Al ₂ O ₃ –TiO ₂ (s) 28.3/71.7/0	Fe, pure	1550	Ar	113.5	[126]
MgO–Al ₂ O ₃ –TiO ₂ (s) 27.5/69.5/3.0	Fe, pure	1550	Ar	116.1	[126]
MgO–Al ₂ O ₃ –TiO ₂ (s) 26.6/67.4/6.0	Fe, pure	1550	Ar	122.1	[126]
MgO–Al ₂ O ₃ –TiO ₂ (s) 25.8/65.2/9.0	Fe, pure	1550	Ar	103.0	[126]
MgO–Al ₂ O ₃ –TiO ₂ (s) 24.9/63.1/12.0	Fe, pure	1550	Ar	120.8	[126]
MgO–Al ₂ O ₃ –TiO ₂ (s) 24.1/60.9/15.0	Fe, pure	1550	Ar	122.8	[126]
MgO–MgO·Al ₂ O ₃ –Al ₂ O ₃ (s) 72.1/27.9/0	Fe, pure	1550	Ar (5% H ₂)	120.4	[123]
MgO–MgO·Al ₂ O ₃ –Al ₂ O ₃ (s) 44.2/55.8/0	Fe, pure	1550	Ar (5% H ₂)	116.7	[123]
MgO–MgO·Al ₂ O ₃ –Al ₂ O ₃ (s) 16.3/83.7/0	Fe, pure	1550	Ar (5% H ₂)	114.2	[123]
MgO–MgO·Al ₂ O ₃ –Al ₂ O ₃ (s) 0/72.7/27.3	Fe, pure	1550	Ar (5% H ₂)	115.9	[123]
CaO–Al ₂ O ₃ (l) 36/64	Fe	1600	–	65	[70]
CaO–Al ₂ O ₃ (l) 50/50	Fe	1600	–	58	[70]
CaO–Al ₂ O ₃ (l) 58/42	Fe	1600	–	54	[70]

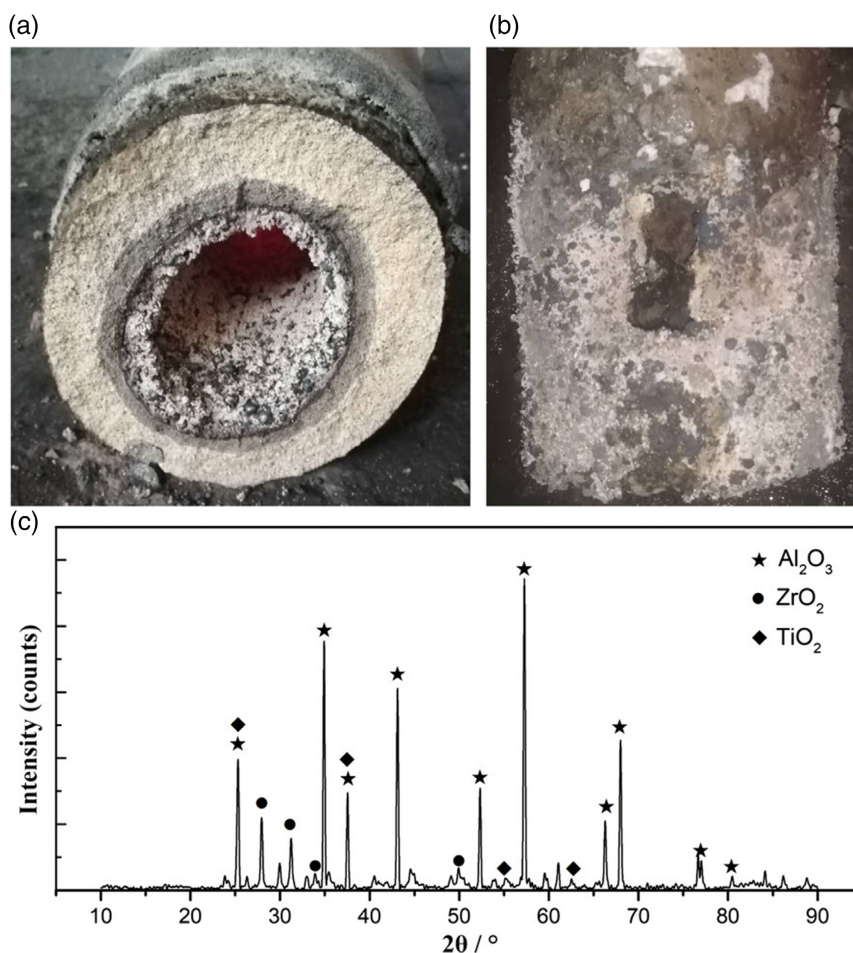


Figure 7. An example of nozzle clogging in a typical IF steel: a) cross-section of the nozzle, b) entry of the nozzle, and c) XRD spectrum of the nozzle clogging. Reproduced with permission.^[72] Copyright 2021, Wiley-VCH GmbH.

the influence of purging, lab-scale experiments provide a detailed insight into the chemical aspects of inclusion reactions and interactions. However, they can focus on isolated reactions and interactions, providing an essential puzzle stone for the overall clogging picture. Additionally, extraction techniques to investigate the 3D characteristics of inclusions have been applied.^[79,81] Ren et al.^[81] proposed a four-step modification mechanism of inclusions during Ca-treatment in line pipe steels. Based on angular shaped Al₂O₃ after deoxidation, a CaS outer layer promptly forms after CaSi addition, followed by the formation of a xCaO.yAl₂O₃ layer generation due to the reaction between Al₂O₃ and CaS or dissolved oxygen. Finally, the Al₂O₃ is fully modified to a spherical calcium aluminate.

A method that is often used to investigate interfacial phenomena such as wettability, reactivity, or surface tension between liquid steel and solid oxides is HT-DSA.^[69,82–84] With this method, the contact angle between two phases can be determined. Subsequent metallographic analyses of the interface can clarify if a reaction product between the two phases has formed. Measured contact angles of steel in contact with different substrates provide essential data for theoretical modeling approaches and numerical simulations of particle behavior at interfaces.

Comparing results of DSA analyses from the literature for different steel/refractory combinations confirms the significant influence of steel and refractory composition on different steel grades' clogging behavior.

In the 1990s, a method for the in situ observation of inclusion reactions was first introduced by Yin et al.^[85]: High-temperature laser scanning confocal microscopy (HT-LSCM) enables the in situ observation of inclusions in contact with steel, slag, and refractory at steelmaking temperatures. One focus concerning clogging is studying the so-called attraction forces between different inclusion types and sizes. In the specific case, Yin et al.^[85,86] analyzed the agglomeration of different inclusion types on a molten steel surface. The authors report that the non-wettability behavior of the alumina-based NMIs generates a deformation of the liquid surface, which is called meniscus. If two particles approach one another, the meniscus between them is further depressed or drawn downward. This change, called capillary attraction, can lead to a difference in capillary pressure between the inside and the outside area of the pair, which will push the two bodies towards each other. The capillary attraction is the source of attraction between alumina inclusions at free surfaces and gas bubbles inside the liquid steel melt.^[86,87] The

Table 2. Investigation of SEN clogging deposits from continuous casting machines.

Steel grade ^{a)}	Ca-treatment	Clogging inducing solid nonmetallic phase	Associated nonmetallic phases and compounds	References
ULC	no	Al ₂ O ₃	– CA ₃ , CA ₄ , CA ₅ , C ₂ A ₇ , MgO	[130]
Ti-ULC	no	Al ₂ O ₃	MA-spinel, Ti ₃ O ₅ TiO _x FeO, TiO ₂ , FeO·Al ₂ O ₃ Al-Mg-Ti-oxide, Al-Ti-Oxide, TiS, TiN MA-spinel, CA ₂ , CA ₆ , CaO·TiO ₂	[28] [20,52,74,130-133] [75] [4] [134]
Ti-stabilized stainless steel	–	MA-spinel Ca-Al-Ti-oxides	Al ₂ O ₃ , Ti ₃ O ₅ ZrO ₂ , SiO ₂	[28] [135]
	no	TiO ₂ , Al ₂ O ₃	Cr ₂ O ₃ , TiN	[136]
	–	TiN	MA-spinel	[48,137]
	yes	CaO·TiO ₂ MA-spinel	MA-spinel –	[137] [137]
LC-AK	no	Al ₂ O ₃	Ca–Si–Al–Mn–oxides MA-spinel –	[73] [28] [2,20,74,138,139]
	yes	CA, MA CA ₂	CA ₂ , CA ₆ , Ca–Mg–Al–Si–oxides CA	[140,141] [28,142]
MC-AK	yes	CA, CA ₂ , CaS CA ₂ , CA ₆	C ₁₂ A ₇ , C ₃ A C ₁₂ A ₇	[143] [143]
	no	Al ₂ O ₃	CaO, MgO	[144,145]
MC-SK	yes	Ca-Si-oxides, CaS	Ca-Al-oxides, Ca-Si-Al-oxides	[58]
MC-ASK	yes	CaS	Ca-Si-Al-oxides	[58]
HC-AK	no	Al ₂ O ₃	FeO·Al ₂ O ₃ , CaO, SiO ₂ , MnO	[73]
Resulfurized steel grades (> 0.02% S)	yes	CaS	C ₁₂ A ₇ , CA, MA-spinel	[28]
		CaS, CA, CA ₂	Calcium aluminates, MA-spinel MA-spinel	[146] [142,147,148]
Rephosphorized steel grades	yes	Al ₂ O ₃ , TiO ₂	–	[72]
		CA ₆	–	[57]

^{a)}IF Interstitial free; ULC Ultra-low carbon; LC Low carbon, MC Medium carbon; HC High carbon; SK Si-killed; AK Al-killed; ASK Al-Si-killed.

Table 3. Summary of experimental methods to investigate the clogging phenomenon.

Topic	Investigated Phases	References
Inclusion behavior post-mortem	Steel/NMI	[77-81,106,149-152]
Wettability	Steel/Refractory/NMI	[52,82,84,153-155]
In-situ inclusion behavior	Liquid Steel/NMI	[64,85-88,90,91,156-163]
	Refractory/Steel/NMI	[88,90,91,164]
Refractory characterization	Stability with Steel	[15,93]
	Erosion and corrosion	[14,20,33,34,165-172]
	Permeability	[21,173]
	Thermochemical Reactions	[92,174]

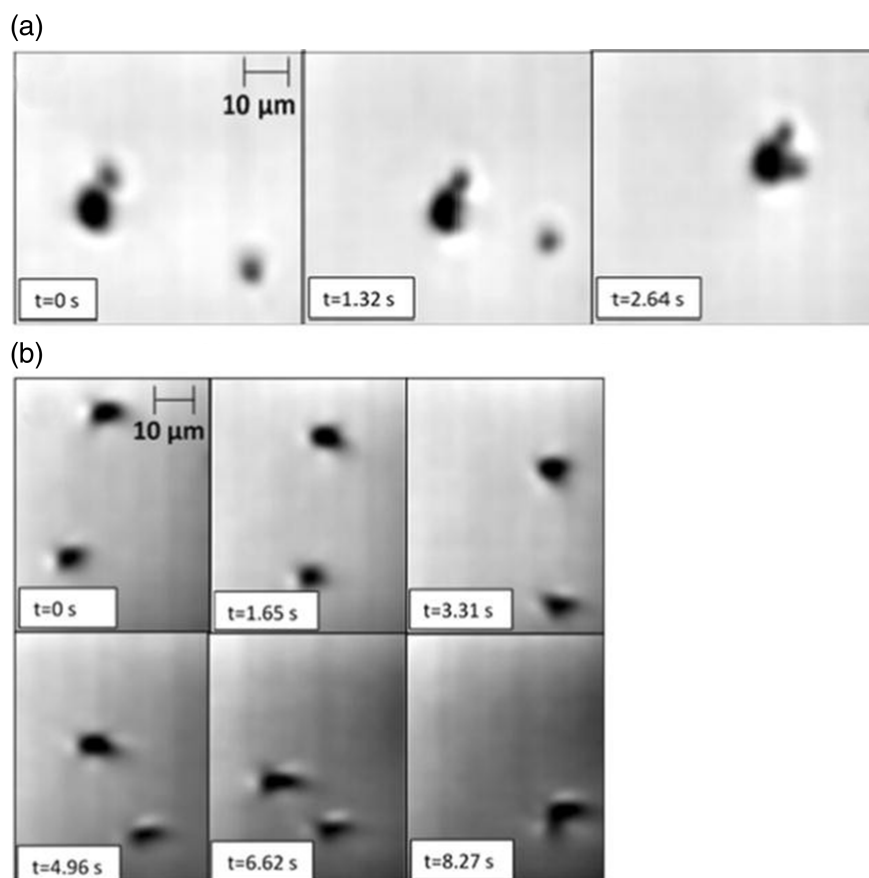


Figure 8. Change in inter-inclusion distance with time for a pair of inclusion particles observed a) Before Ca-treatment and b) After Ca-treatment. Reproduced under terms of the CC-BY license.^[89] Copyright 2017, The Authors, published by Springer Nature.

magnitude of the attraction force is calculated based on measured particle acceleration in confocal experiments and estimated particle mass. Several studies using the same approach for observation and evaluation followed. It is agreed in the literature that the agglomeration tendency for liquid and semi-liquid inclusions is smaller than for solid inclusions.^[88,89] The attraction force of a pair of semi-liquid particles containing Ca was determined with approximately 10^{-16} – 10^{-15} N by Michelic et al.^[90] compared to solid alumina inclusion with attraction forces in the range 10^{-14} – 10^{-15} N.^[88] This difference in attraction force again explains the main reason for the Ca-treatment as an effective countermeasure against clogging for various steel grades. **Figure 8** effectively illustrates an example of in situ observations of the agglomeration tendency of inclusions before and after Ca-treatment. Also, the steel/refractory interface has already been part of in situ investigations.^[88,90,91] It can be summarized that LSCM data supplies valuable at least qualitative data regarding the inclusion behavior at different interfaces.

Refractory characterization is done by various well-established methods, from the classical refractory immersion or dipping test,^[14,17,33,92] where refractories are immersed in a melt held, e.g., in an induction furnace. The refractory usually rotates inside the melt resulting in build-up formation on the refractory. Another option is a static accretion or crucible experiment,^[15,93]

where crucibles are produced from specific refractory parts to study their interaction with the steel. Both experiment types aim at the stability of the refractory material and to characterize steel/refractory interaction. Stable and well controllable experimental conditions are fundamental to providing relevant data for further evaluation. Additionally, qualitative information on the erosion and corrosion of different nozzle materials is obtained.

3.3. Theoretical Consideration of Particle Deposition at the Steel/Refractory Interface

In principle, when two spherical inclusions approach each other in molten steel, they tend to agglomerate to form larger particles due to interfacial contact forces and to reduce their surface energy. The procedure of inclusion deposition at the steel/refractory interface is explained similarly^[94] and is divided into three steps: transport, adhesion, and sintering. These different steps are schematically illustrated in **Figure 9**. First, inclusions are transported from the bulk region to the boundary layer and may eventually get in contact with the nozzle refractory. Second, inclusions adhere to the refractory wall due to interfacial forces, potentially leading to a cavity formation around the

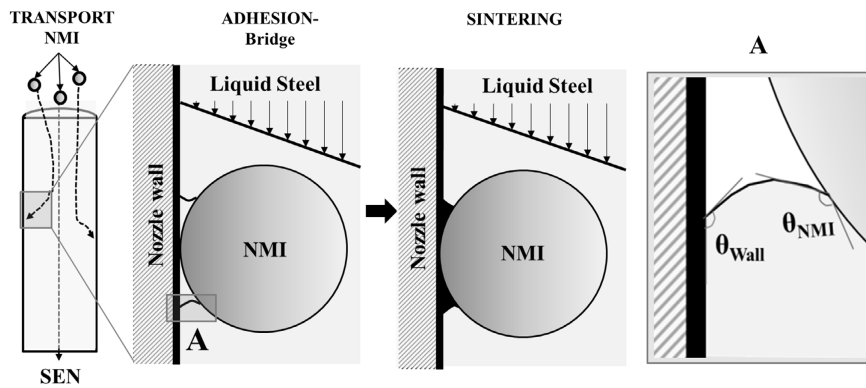


Figure 9. Different steps of the deposition process of nonmetallic inclusion (NMI) transported from the bulk flow region into the boundary layer at the steel/refractory interface. Reproduced with permission.^[100] Copyright 2018, Springer Nature.

Table 4. Summary of the research done about NMI deposition at a steel/refractory interface, adapted with permission from Ref.^[100] copyright 2018, springer-verlag GmbH.

Deposition Step	Description	Reference
Transport		
x	General description of the process steps; boundary layer theory	[10]
x	Local eddy transport phenomena	[175]
x	Local eddy transport phenomena	[11]
	Filtration mechanism of NMI in steel at a ceramic filter	[97]
	Al ₂ O ₃ adhesion at a nozzle with steel reoxidation	[94,98]
	NMI filtration in molten steel	[176]
	Influence of iron oxides on the adhesion force	[99]
	Effect of inclusion morphology on adhesion force	[150]
	Attraction force of Al ₂ O ₃ particle agglomerations in the melt	[177]

contact point (see Detail A in Figure 9). The cavity might be filled with gaseous components from the steel or the refractory, melt vapor, or liquid phases forming due to a local rise in the oxygen concentration. Finally, a solid structure forms due to the sintering of inclusions at the interface. The literature agrees about the deposition of inclusions on the refractory wall during casting, but discussions regarding the governing mechanism are still ongoing. **Table 4** summarizes some of the research done on the deposition of inclusions at interfaces in the steel. The boundary layer theory proposed by Singh et al.^[10] and the local eddy transport phenomenon^[11,95] dominate particle transport. As described previously, the contact angle between Al₂O₃ and liquid iron is $\approx 137^\circ$,^[10,70] a non-wetting situation, respectively. So, when the contact angle between inclusion and the steel is high, the adherence between inclusion and refractory will also increase, explaining the distinct clogging tendency of solid Al₂O₃ particles. Sintering will start immediately after the first particle contact considering the high temperatures.

The adhesion step is governed by the interfacial properties between steel, refractory, and inclusion. Establishing a theoretical modeling approach for the adhesion of a particle at the steel/refractory interface, attractive forces, and potential forces contributing to the detachment of the particle must be considered.

Adhesion and van der Waals forces are most discussed for this issue as attractive forces, while buoyancy, drag, and lift forces are named as detachment forces. The equation still predominantly applied as the basis for the adhesion force description has already been expressed by Fisher^[96] in 1926. As described in Equation (2), the adhesion force F_A is a function of the surface tension of the molten steel σ , R_2 is the radius at the thinnest point of the neck of fluid connecting the two bodies (see Figure 9, Detail A) and ΔP is the pressure difference between the steel and the cavity phase.^[94,97–99] The mechanical equilibrium of the bridge interface is given by the Young–Laplace equation, which relates the pressure difference across the interface to both the mean curvature of the interface and the interfacial tension between the contacting fluids (Equation (3)), where R_1 and R_2 are the cavity radii.^[100–103]

$$F_A = 2\pi R_2 \sigma + \pi R_2^2 \Delta P \quad (2)$$

$$\Delta P = \sigma \left(\frac{1}{R_1} - \frac{1}{R_2} \right) \quad (3)$$

Based on these assumptions, Dieguez-Salgado et al.^[100] presented a theoretical model for describing this force balance

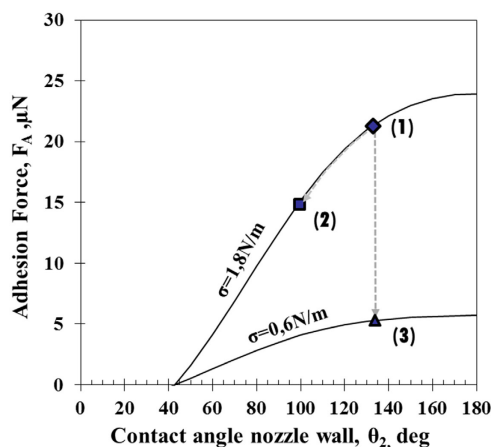


Figure 10. Model calculation illustrating the relation between adhesion force, the surface tension of molten steel, and the nozzle wall's contact angle. Reproduced with permission.^[100] Copyright 2018, Springer Nature.

and the situation of a NMI at the steel/refractory interface. One of the obtained results is illustrated in **Figure 10**. In the presented case, the adhesion force is calculated between an Al_2O_3 inclusion with $5\ \mu\text{m}$ in diameter and an alumina-based refractory wall (point 1 in **Figure 10**). Points 2 and 3 represent two possible options to decrease the adhesion force in the system. In point 2, the adhesion force is lowered due to a new nozzle material with a better wettability for liquid steel than the alumina-based one. A zirconia-based material with a contact angle of $\approx 100^\circ$ was used for this calculation. Although the influence of wettability is clearly demonstrated, it has to be kept in mind that refractories with good wettability with liquid steel often also exhibit a higher reactivity with the steel phase. This is especially true for nozzle materials with a contact angle in the range of 40° – 60° .^[104] So, a nozzle material combining the effect of a decreased adhesion force, on the one hand, and potentially low reactivity, on the other hand, is desired. In industrial practice, so-called anti-clogging layers are applied to prevent the appearance of clogging. **Table 5** summarizes some observations from the literature regarding the application of different layers and the associated mechanisms behind them.

Another interesting approach has been published by Cheng et al.^[105] in their study on the clogging behavior of an

SEN for the casting of Ca-treated Al-killed Ti-bearing steels. The formation of an initial layer on the inner nozzle wall was observed due to inclusion adhesion. In a second step, the adhered particles reacted with the refractory material forming a low-melting-point reaction layer. This layer finally penetrated the nozzle material resulting in the damage of the nozzle material as a consequence of the good wettability between the interaction layer and the nozzle material.

Referring to point 3 in **Figure 10**, another option to reduce the adhesion force is a decreased surface tension between the steel and the fluid phase inside the cavity. Various authors suggested that FeO particles could act as a binder for the alumina particles.^[94,99] In such a case, the adhesion force is significantly reduced, assuming a liquid bridge between the inclusion and the nozzle wall. Since this case might not be common in industrial practice, it can be seen as an approximation for the use of lime-bearing or calcium-zirconate nozzles. A further reduction of the adhesion force will be reached if the inclusion changes from solid to semi-liquid or even liquid state. The latter again confirms the significance of Ca-treatment to avoid clogging for defined steel grades. However, for reasons of completeness, it should be mentioned that Ca-treatment is not possible for every steel grade, primarily due to the high reactivity of Ca with slag components, which only allows a successful Ca-treatment for selected plant configurations and metallurgical practices. One group of steels, which is usually not Ca-treated, are Ti-ULC and IF-steels.

4. Clogging Tendency for the Example of Ti-ULC Steels

Ti-stabilized ULC steels are widely used in the automotive industry for body part applications. However, these steels are well known for their distinct clogging tendency in the SEN. This is often attributed to the necessary addition of titanium used as a stabilizer for the residual carbon and nitrogen content.^[76,106] The typical production route for these steels in an integrated steel mill is via Ruhrstahl Heraeus (RH) treatment. A high oxygen activity in the range of 500–700 ppm is necessary to ensure proper decarburization during RH-degassing. Ca-treatment is usually not recommended due to high FeO contents in the secondary steelmaking slag of around 20 wt%. Despite the dissolution of deoxidation products after the RH treatment,

Table 5. Summary of proposed materials for anti-clogging layers in the submerged entry nozzle.

Material	Reference	Fundamental mechanism of clogging prevention
Lime-bearing nozzles	[2,178,179]	
Calcium zirconate	[169,180-183]	Reaction of CaO in refractory with alumina inclusions to form an oxide phase with low melting point and high wettability, resulting in a decrease of the attractive force and the prevention of solid deposits.
Calcium titanate	[93,183,184]	
SiAlON	[34,185]	
Boron nitride	[186]	Formation of boron oxide-rich low melting phases due to reaction of BN with entrapped oxygen and/or oxides. Prevention of solid deposits at the steel/refractory interface. Additionally, prevention of steel infiltration due to poor wettability of BN;
Silica- and C-free layers	[187-189]	Elimination of steel reoxidation at the steel/refractory interface due to the prevention of CO-formation resulting from the reaction between C and SiO_2 at high temperatures. Additionally, C-free layers reduce the heat loss of the steel in the SEN and prevent it from freezing.

the FeO-content stays high until casting, which can cause significant reoxidation and losses of dissolved aluminum. Burty et al.^[107] have reported of high losses of dissolved Al and Ti ($\Delta c \approx -150$ ppm) during the changeover period of the ladle due to reoxidation by the ladle slag, which finally led to the rejection of the slabs as the composition did not meet the requirements. One possibility is to reduce the slag by adding CaC_2 or additives containing metallic Al to the slag, which has been reported to limit the FeO content to 2.5–5%.^[108] Cicutti et al.^[57] analyzed the recovery rate of calcium depending on the FeO-content of the ladle slag. 2.5% FeO already lead to a remarkable decrease of the Ca-recovery which involves the danger of uncontrollable Ca-content and incomplete inclusion modification resulting in an increased clogging tendency. In general, it is demonstrated that the overall FeO + MnO concentration in the slag should not exceed 8%. At the end of decarburization, the remaining dissolved oxygen is killed by Al-addition, aiming a final content of 300–500 ppm Al. Ti-addition and homogenization of the melt are the last steps before casting.^[108]

The investigation of clogging deposits of Ti-ULC melts presents contrasting results. An overview of different observations has already been introduced in Table 2. In most cases, mainly Al_2O_3 clusters form the clogging network. But also at least traces of Ti-rich phases were frequently observed. Cui et al.^[75] reported the presence of $\text{FeO}\cdot\text{TiO}_2$ and $\text{Al}_2\text{O}_3\cdot\text{TiO}_2$ in the clogged material acting as a binder phase between the Al_2O_3 particles. Ti-containing phases were often accompanied by solidified steel inside the clogged material due to an increased wettability of $\text{Al}_2\text{O}_3\text{--TiO}_x$ inclusions. Although significant research has been done in Ti-ULC, the reason and mechanisms for their increased

clogging tendency are still not fully understood, and several aspects have to be considered. One crucial point consistent in the literature is that the deposition of alumina particles coming from deoxidation is seen as the decisive mechanism for clogging. The Ti-addition results in an increased wettability between steel and the inclusions,^[82,109] finally leading to a reduced driving force for particle agglomeration and lower inclusion removal rates from the melt. This further implies a higher number of small particles in the melt during casting.^[52,88] These small inclusions are assumed to be more harmful than larger inclusions and are commonly seen as the main reason for the clogging sensitivity of Ti-alloyed ULC-steel.

Al_2O_3 should be the dominating stable phase in Ti-ULC steels from a thermodynamic viewpoint.^[77,78,110] However, it was reported that a potential change in thermodynamic conditions due to a local loss of soluble Al could cause the formation of Ti-containing inclusions.^[111,112] Nevertheless, heterogeneous $\text{Al}_2\text{O}_3\text{--TiO}_x$ inclusions are found by various researchers.^[113,114] Usually, they are described as a dense alumina shell around a Ti-rich core. Kang et al.^[112] provided a thermodynamic reassessment of the system Fe-Al-Ti-O. The authors proposed a new oxide stability diagram showing a stable region of liquid oxides in the system. In recent work, Park et al.^[115] studied the influence of oxygen partial pressure on the phase equilibria of the $\text{Al}_2\text{O}_3\text{--TiO}_x$ system providing an essential basis for a deepened understanding of inclusion evolution in Ti ULC steels. **Figure 11** shows some of the results of this work. It can be seen that the solubility of Ti oxide in the corundum decreases with increasing $p\text{O}_2$ and that the stable region of the pseudobrookite is shifted towards the Ti-oxide-rich side with decreasing $p\text{O}_2$.

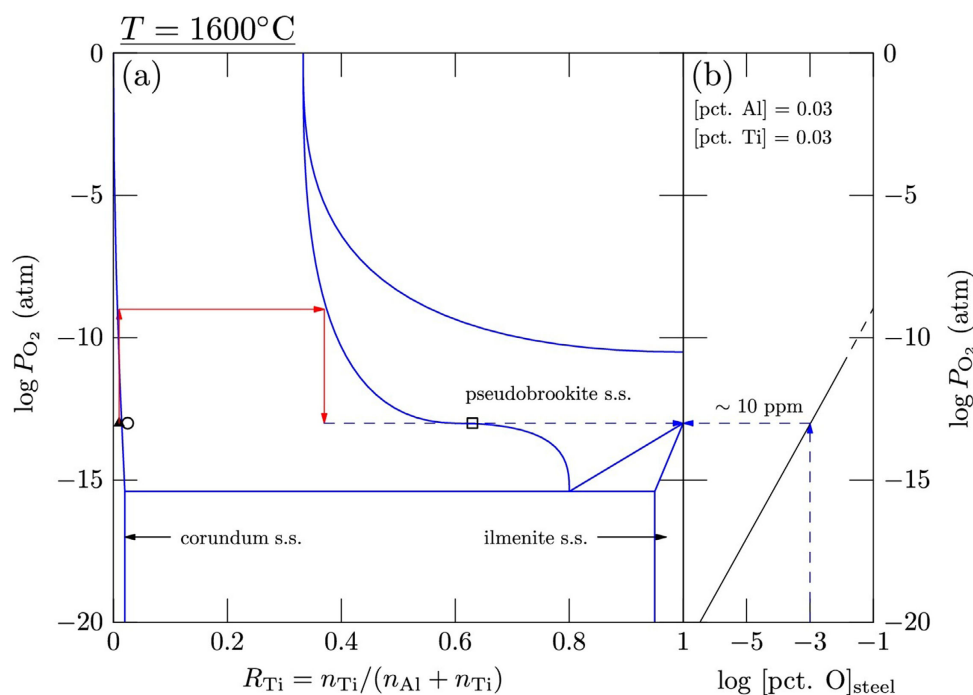


Figure 11. a) Estimated phase diagram of Al-Ti-O₂ at 1600 °C based on experimental data and b) calculated equilibrium O content in liquid steel containing 0.03% Al and 0.03% Ti. Reproduced with permission.^[115] Copyright 2021, Elsevier

The authors concluded that reoxidation plays a vital role in this system's inclusion behavior. The oxygen potential of the steel system rapidly increases, enabling the change of an Al_2O_3 inclusion to another phase. However, once the transformed inclusions are re-entrapped into the steel, the inclusions transform again due to low oxygen potential inside the melt. This finally can explain the instability of Al_2TiO_5 assuming reducing conditions and that the pseudobrookite phase could be an additional source for inclusion formation in the steel melt.

Another aspect discussed in the literature is the local supersaturation of Ti shortly after Ti-addition. The latter might also lead to transient inclusion formation. In this context, different authors especially indicate a morphology change of Al_2O_3 inclusions responsible for the appearance of clogging. Inclusion morphology can be controlled by adjusting the Ti/Al ratio.^[77,78,116] As a last aspect, FeTi quality is essential in laboratory and industrial trials. FeTi was identified as an additional source for bringing oxygen to the system and significantly changing the thermodynamic conditions.^[76,117] The following measures are suggested in the literature to avoid or at least possibly control the appearance of clogging in Ti-ULC steels^[69,76,115]: 1) Decrease of Ti-content: The necessary Ti-content is mainly based on the residual amount of dissolved carbon and nitrogen. Effective vacuum treatment during decarburization results in a lower Ti-content, which is needed to bind nitrogen and carbon during solidification and cooling; 2) Decrease of the Ti/Al-ratio: A lower Ti/Al-ratio minimizes the number of inclusions modified to particles in the system Al-Ti-O. The reduction of the Ti/Al-ratio should be realized by an increase of the [Al]-content; 3) Increase of time between Al-killing and FeTi-addition: The lapse time between Al-killing and FeTi-addition should be as long as possible to increase the cleanliness of the steel before the FeTi-addition. The fewer inclusions are present at the time of FeTi-addition, the fewer particles can be modified; 4) Sufficient time between FeTi-addition and the start of casting: The FeTi-addition causes the formation of transient inclusions. Sufficient time is necessary for the inclusions to react towards a stable state; and 5) Control of the FeTi-quality: The FeTi is a significant source of oxygen. In the case of FeTi-addition, a new population of Ti-containing alumina-based inclusions nucleates. These particles will be attracted by the interface and increase the tendency towards clogging.

5. Future Demands and Perspectives of Clogging Related Research

The presented state of the art on the significance of NMIs regarding the clogging phenomenon confirms the common understanding that the wetting angle between steel and NMIs or refractory materials is the dominating influencing factor for adhesion and agglomeration phenomena. Significant knowledge has been established and tremendous progress has been achieved in understanding the various mechanisms and related influence parameters on the appearance of clogging. Specific countermeasures have been deduced and their scientific background has been evaluated in detail. The investigation of clogged material from industry and the observation of defined reactions and interactions in the system steel-refractory-inclusions on laboratory scale noticeably contributed to advancing the

understanding of this phenomenon. However, the sensitivity of specific steel grades is still valid and not entirely eliminated. Research on various aspects is still ongoing. It is essential that although the isolated observation of particular reactions and mechanisms is very beneficial, a comprehensive view from different positions and research disciplines is needed to understand the clogging problem in its entirety.

The crude transformation in steelmaking toward hydrogen-based crude steel production will also influence the future levels of trace and tramp elements in the steel. Their influence on wetting characteristics is partly unknown and therefore part of ongoing research.^[118] Also, the role of rare-earth elements is the focus of researchers today. Applied initially as tracer material to track the inclusions from deoxidation over subsequent process steps until casting,^[119] their influence on interfacial reactions in the system steel-slag-refractory-inclusion is currently under investigation^[120] and will be important in the future. In this perspective, the quality of alloying elements will also remain a major aspect to control, e.g., oxygen levels in the liquid steel. Ongoing process optimization and artificial intelligence approaches will provide a considerable amount of data and diverse options for process monitoring and optimization.

Nevertheless, clogging will not completely disappear as it is still an ensemble of various complex reactions. Some questions remain unsolved so far, and detailed explanations on why steel tends to clog in one case and not in the other, even if process conditions and steel compositions are apparently the same, cannot be fully answered. The appearance of clogging incidences at rare intervals makes it statistically again more challenging. Taking all these boundary conditions, the clogging problem will remain on the to-do list of steelmakers, refractory suppliers, and researchers to figure out the best solutions for the specific customer setting.

Acknowledgements

The work of Uxia Dieguez-Salgado, Philipp Dorner and Augustin Karasangabo performed during their Ph.D. theses on clogging-related topics is greatly acknowledged. The authors gratefully acknowledge the funding support of K1-MET GmbH, metallurgical competence center. The research program of the K1-MET competence center is supported by COMET (Competence Center for Excellent Technologies), the Austrian program for competence centers. COMET is funded by the Federal Ministry for Climate Action, Environment, Energy, Mobility, Innovation and Technology, the Federal Ministry for Digital and Economic Affairs, the provinces of Upper Austria, Tyrol, and Styria, and the Styrian Business Promotion Agency (SFG). The financial support by the Austrian Federal Ministry for Digital and Economic Affairs, the National Foundation for Research, Technology and Development and the Christian Doppler Research Association is gratefully acknowledged.

Conflict of Interest

The authors declare no conflict of interest.

Keywords

adhesion, clogging, contact angle, deposition, nonmetallic inclusions, refractory wall, wetting

Received: January 31, 2022
Revised: March 15, 2022
Published online: April 5, 2022

- [1] K. Rackers, B. G. Thomas in *Proc. of the 78th Steelmaking Conf.*, Iron and Steel Society, Nashville, TN, April 1995, p. 723; Society, Warrendale, PA, Vol. 78, 1995, pp. 723-734
- [2] S. Ogiyayashi, *Taikabutsu Overseas* **1995**, 15, 3.
- [3] R. Dekkers, *PhD Thesis, Katholieke Universiteit Leuven* **2002**.
- [4] W. Tiekink, A. Overbosch, G. Abel, W. Damen, in *Proc. of the 9th Clean Steel Conf.*, Budapest, September 2015, p. 1.
- [5] R. B. Snow, J. A. Shea, *J. Am. Ceram. Soc.* **1949**, 32, 187.
- [6] G. C. Duderstadt, R. K. Iyengar, J. M. Matesa, *JOM* **1968**, 20, 89.
- [7] H. Bai, B. G. Thomas, in *Proc. of the 83rd Steelmaking Conf.*, Iron and Steel Society, Pittsburgh, PA, March 2000, p. 2.
- [8] D. Janke, Z. Ma, P. Valentin, A. Heinen, *ISIJ Int.* **2000**, 40, 31.
- [9] F. L. Kerneny, in *Proc. of the Mc Lean Symp.*, Iron and Steel Society, Toronto, CA July 1998, p. 103.
- [10] S. N. Singh, *Metall. Trans.* **1974**, 5, 2165.
- [11] S. Dawson, *Iron Steelmaker* **1990**, 17, 33.
- [12] M. Andersson, O. Wijk, in *Proc. of Scaninjet VI: 6th Int. Conf. on Refining Processes*, Lulea, June 1992, p. 175.
- [13] M. Nadif, J. Lehmann, M. Burty, J.-F. Domgin, *Rev. Met. Paris* **2007**, 104, 493.
- [14] Y. Fukuda, Y. Ueshima, S. Mizoguchi, *ISIJ Int.* **1992**, 32, 164.
- [15] S. Ramachandran, K. D. Peaslee, J. D. Smith, in *Proc. of the 84th Steelmaking Conf.*, Iron and Steel Society, Baltimore, MD March 2001, p. 729.
- [16] N. Kasai, M. Kawasaki, Y. Hayashi, H. Kawai, *Taikabutsu Overseas* **1990**, 11, 22.
- [17] H. Shikano, T. Harada, S. Iitsuka, S.-I. Kataoka, *Taikabutsu Overseas* **1990**, 11, 10.
- [18] J. Poirier, B. Thillou, M. A. Guiban, G. Provost, in *Proc. of the 78th Steelmaking Conf.*, Iron and Steel Society, Nashville, TN April 1995, p. 451.
- [19] R. B. Tuttle, K. D. Peaslee, J. D. Smith, in *Proc. of the AISTech 2004*, AIST—Association for Iron & Steel Technology, Nashville, TN September 2004, p. 669.
- [20] Y. Hiraga, Y. Yashima, K. Fujii, *Taikabutsu Overseas* **1994**, 15, 22.
- [21] M. Suzuki, Y. Yamaoka, N. Kubo, M. Suzuki, *ISIJ Int.* **2002**, 42, 248.
- [22] S. M. Göklü, K. W. Lange, *Arch. Eisenhüttenwesen* **1984**, 55, 9.
- [23] P. R. Scheller, S. Lachmann, in *Proc. of the Unitecr '07*, Dresden September 2007, p. 334.
- [24] J. W. Farrell, D. C. Hilty, in *Proc. of the 29th Electric Furnace Conf.*, Toronto, CA, December 1971, p. 31.
- [25] M. Anderson, O. Wijk, in *Proc. of the 6th Inter. Conf. on Refining Processes*, Lulea, Sweden June 1992, p. 175.
- [26] H. Barati, M. Wu, A. Kharicha, A. Ludwig, *Steel Res. Int.* **2020**, 91, 2000230.
- [27] N. Bannenberg, in *Proc. of the 78th Steelmaking Conf.*, Iron and Steel Society, Nashville, TN April 1995, p. 457.
- [28] W. Fix, H. Jacobi, K. Wünnenberg, *Steel Res.* **1993**, 64, 71.
- [29] S. R. Story, G. E. Goldsmith, G. L. Klepzig, *Rev. Met. Paris* **2008**, 105, 272.
- [30] H. Ling, L. Zhang, H. Li, *Metall. Mater. Trans. B* **2016**, 47, 2991.
- [31] S. Chang, Z. Zou, J. Liu, M. Isac, X. E. Cao, X. Su, R. I. L. Guthrie, *Powder Technol.* **2021**, 387, 125.
- [32] Q. Fang, H. Zhang, R. Luo, C. Liu, Y. Wang, H. Ni, *J. Mater. Res. Technol.* **2020**, 9, 347.
- [33] M. Nakamura, T. Kiwada, O. Nomura, K. Ichikawa, *Taikabutsu Overseas* **1995**, 15, 28.
- [34] W. Zhong, W. Li, X. Zhong, in *Proc. of the Int. Symp. on Advances in Refractories for the Metallurgical Industries II*, Montreal, CA, August 1996, p. 441.
- [35] P. Andrzejewski, K. U. Kohler, W. Pluschkell, *Steel Res.* **1992**, 63, 242.
- [36] U. Horbach, S. Rödl, H. Abratis, F. Höfer, *Stahl Eisen* **1995**, 115, 71.
- [37] G. F. Wilson, J. M. Heesom, A. Nichilson, A. W. Hills, *Ironmaking Steelmaking* **1987**, 14, 296.
- [38] Y. Yang, P. G. Jönsson, M. Ersson, K. Nakajima, *Steel Res. Int.* **2015**, 86, 341.
- [39] B. G. Thomas, L. Zhang, *ISIJ Int.* **2001**, 41, 1181.
- [40] B. G. Thomas Zhang, in *Proc. of the 14th National Steelmaking Symp.*, Morelia, November 2003, p. 138.
- [41] S. Sivaramkrishnan, H. Bai, B. G. Thomas, S. P. Vanka, P. H. Dauby, M. Assar, in *Proc. of the 59th Ironmaking Conf.*, Iron and Steel Society, Pittsburgh, PA, March 2000, p. 541.
- [42] O. Araromi, B. G. Thomas, E. Conzemius, in *Proc. of the Materials Science and Technology Conf.*, AIST/TMS, Pittsburgh, PA October 2009.
- [43] H. Bai, B. G. Thomas, *Metall. Mater. Trans. B* **2001**, 32B, 253.
- [44] Q. Xie, M. Nabeel, M. Ersson, P. Ni, *Steel Res. Int.* **2022**, 93, 2100410.
- [45] H. Barati, M. Wu, A. Kharicha, A. Ludwig, *Powder Technol.* **2018**, 329, 181.
- [46] H. Barati, M. Wu, S. Michelic, S. Ilie, A. Kharicha, A. Ludwig, Y.-B. Kang, *Metall. Mater. Trans. B* **2021**, 4167.
- [47] S. K. Michelic, D. Loder, T. Reip, A. Ardehali Barani, C. Bernhard, *Mater. Charact.* **2015**, 100, 61.
- [48] R. Maddalena, R. Rastogi, S. Bassem, A. W. Cramb, *Iron Steelmaker* **2000**, 27, 71.
- [49] P. Dorrer, S. K. Michelic, G. Klösch, J. Reiter, A. Paul, C. Bernhard, in *Proc. of the AISTech2017*, AIST—Association for Iron & Steel Technology, Nashville, TN May 2017, p. 1555.
- [50] T. Bolender, J. Cappel, K. Wünnenberg, W. Pluschkell, *Steel Res.* **2001**, 72, 477.
- [51] P. Valentin, A. Heinen, S. Landa, D. Janke, Z. Ma, *European Commission, Luxembourg*, **2001**, EUR 19486.
- [52] C. Bernhard, G. Xia, M. Egger, A. Pissenberger, S. K. Michelic, in *Proc. of the AISTech2012*, AIST—Association for Iron & Steel Technology, Atlanta, GA May 2012, p. 2191.
- [53] A. Karasangabo, C. Bernhard, *BHM* **2004**, 149, 83.
- [54] K. C. Mills, S. Sridhar, in *Proc. of the Belton Memorial Symp.*, Sydney January 2000, p. 211.
- [55] W. V. Bielefeldt, A. C. F. Vilela, *Steel Res. Int.* **2015**, 86, 375.
- [56] C. E. Cicutti, J. Madias, J. C. Gonzales, *Ironmaking Steelmaking* **1997**, 24, 155.
- [57] C. E. Cicutti, M. Valdez, T. Pérez, R. Ares, R. Panelli, J. Petroni, in *Proc. of the 84th Steelmaking Conf.*, Iron and Steel Society, Baltimore, MD, March 2001, p. 871.
- [58] H. M. Piolet, D. Bhattacharya, *Metall. Mater. Trans. B* **1984**, 15B, 743.
- [59] Y. Higuchi, M. Numata, S. Fukagawa, K. Shinme, *ISIJ Int.* **1996**, 36, 151.
- [60] N. Verma, P. Pistorius, R. J. Fruehan, M. Potter, M. Lind, S. R. Story, *Metall. Mater. Trans. B* **2011**, 42B, 711.
- [61] M. K. Sardar, S. Mukhopadhyay, U. K. Bandopadhyay, S. K. Dhua, *Steel Res.* **2007**, 78, 136.
- [62] C. Liu, Y. Kacar, B. Webler, P. C. Pistorius, *Metall. and Mater. Trans. B* **2021**, 52, 2837.
- [63] H.-Y. Zheng, S.-Q. Guo, M.-R. Qiao, L.-B. Qin, X.-J. Zou, Z.-M. Ren, *Adv. Manuf.* **2019**, 7, 438.
- [64] S. K. Michelic, U. Diéguez-Salgado, D. Loder, C. Bernhard, *Gießerei Praxis* **2016**, 9, 337.
- [65] X. Fan, L. Zhang, Y. Ren, W. Yang, S. Wu, *Metals* **2022**, 2, 181.
- [66] N. Verma, P. C. Pistorius, R. J. Fruehan, M. Potter, M. Lind, S. R. Story, *Metall. Mater. Trans.* **2011**, 42, 720.

- [67] Y. Li, T. Zhang, H. Duan, *Metals* **2019**, 9, 104.
- [68] G. Hassal, K. Mills, *European Commission*, Luxembourg, **1998**. EUR 17894.
- [69] U. Diéguez-Salgado, P. Dorrer, S. K. Michelic, C. Bernhard, *J. Mater. Eng. Perform.* **2018**, 27, 4983.
- [70] A. W. Cramb, I. Jimbo, in *Proc. of the W.O. Philbrook Memorial Symp. Conf.*, Toronto, CA, April **1998**, p. 259.
- [71] K. G. Rackers, *Master Thesis*, University of Illinois **1995**.
- [72] Y. Li, Y. He, Z. Ren, Y. Bao, R. Wang, *Steel Res. Int.* **2021**, 92, 2000581.
- [73] Y. Vermeulen, B. Coletti, B. Blanpain, P. Wollants, J. Vleugels, *ISIJ Int.* **2002**, 42, 1234.
- [74] S. Basu, S. K. Choudhary, N. U. Girase, *ISIJ Int.* **2004**, 44, 1653.
- [75] H. Cui, Y. P. Bao, M. Wang, W. Wu, *Int. J. Miner. Metall. Mater.* **2010**, 17, 154.
- [76] P. Dorrer, S. K. Michelic, C. Bernhard, A. Penz, R. Rössler, *Steel Res. Int.* **2019**, 90, 1800635.
- [77] C. Wang, N. T. Nuhfer, S. Sridhar, *Metall. Mater. Trans. B* **2010**, 41B, 1084.
- [78] H. Matsuura, C. Wang, G. Wen, S. Sridhar, *ISIJ Int.* **2007**, 47, 1265.
- [79] L. Zheng, A. Malfiet, P. Wollants, B. Blanpain, M. Guo, *ISIJ Int.* **2015**, 55, 1891.
- [80] G. Yang, X. Wang, *ISIJ Int.* **2015**, 55, 126.
- [81] Y. Ren, L. Zhang, S. Li, *ISIJ Int.* **2014**, 54, 2772.
- [82] A. Karasangabo, C. Bernhard, *J. Adhes. Sci. Technol.* **2012**, 26, 1141.
- [83] C. Xuan, H. Shibata, S. Sukenaga, P. G. Jönsson, K. Nakajima, *ISIJ Int.* **2015**, 55, 1882.
- [84] S. Ueda, H. Shi, X. Jiang, H. Shibata, A. W. Cramb, *Metall. Mater. Trans. B* **2003**, 34, 503.
- [85] H. Yin, H. Shibata, T. Emi, M. Suzuki, *ISIJ Int.* **1997**, 37, 946.
- [86] H. Yin, H. Shibata, T. Emi, M. Suzuki, *ISIJ Int.* **1997**, 37, 936.
- [87] S. Vantilt, B. Coletti, B. Blanpain, J. Franssaer, P. Wollants, S. Sridhar, *ISIJ Int.* **2004**, 44, 1.
- [88] U. Diéguez-Salgado, S. K. Michelic, C. Bernhard, *IOP Conf. Ser.: Mater. Sci. Eng.* **2016**, 119, 1.
- [89] B. Khurana, S. Spooner, M. B. V. Rao, G. G. Roy, P. Srirangam, *Metall. Mater. Trans. B* **2017**, 48, 1409.
- [90] S. K. Michelic, U. Diéguez-Salgado, C. Bernhard, *IOP Conf. Ser.: Mater. Sci. Eng.* **2016**, 143, 1.
- [91] C. G. Aneziris, C. Schroeder, U. Fischer, H. Berek, M. Emmel, J. Kortus, L. G. Amirkhanyan, T. Weißbach, *Adv. Eng. Mater.* **2013**, 15, 1168.
- [92] A. Memarpour, V. Brabie, P. G. Jönsson, *Ironmaking Steelmaking* **2011**, 38, 229.
- [93] R. B. Tuttle, J. D. Smith, K. D. Peaslee, *Metall. Mater. Trans. B* **2005**, 36B, 885.
- [94] K. Sasai, Y. Mizukami, *ISIJ Int.* **2001**, 41, 1331.
- [95] F. G. Wilson, M. J. Heeson, J. D. W. Rawson, *European Commission*, Luxembourg, **1996**, EUR 11201.
- [96] R. A. Fisher, *J. Agri. Sci.* **1926**, 16, 492.
- [97] K. Uemura, M. Takahashi, S. Koyama, M. Nitta, *ISIJ Int.* **1992**, 32, 150.
- [98] K. Sasai, *ISIJ Int.* **2014**, 54, 2780.
- [99] T. Mizoguchi, Y. Ueshima, M. Sugiyama, K. Mizukami, *ISIJ Int.* **2013**, 53, 639.
- [100] U. Diéguez-Salgado, C. Weiß, S. K. Michelic, C. Bernhard, *Metall. Mater. Trans. B* **2018**, 49, 1632.
- [101] D. Rossetti, S. J. R. Simons, *Powder Technol.* **2003**, 130, 49.
- [102] U. Diéguez-Salgado, *PhD Thesis*, Montanuniversität Leoben **2018**.
- [103] G. Lian, C. Thornton, M. J. Adams, *J. Colloid Interface Sci.* **1993**, 161, 138.
- [104] M. Nadif, M. Burty, H. Soulard, M. Boher, C. Pusse, J. Lehmann, F. Meyer, *IISI Study On Clean Steel*, International Iron and Steel Institute, Brussels **2004**.
- [105] L. Cheng, L. Zhang, Y. Ren, W. Yang, *Metall. Mater. Trans. B* **2021**, 52, 1186.
- [106] P. Kaushik, D. Kruse, M. Ozgu, *Rev. Met. Paris* **2008**, 105, 92.
- [107] M. Burty, L. Peeters, E. Perrin, S. Münzer, P. Colucci, D. Salvadori, F. Schadow, J.-M. Valcarcel, J. Claes, *Rev. Met. Paris* **2005**, 102, 745.
- [108] A. Jungreithmeier, E. Pissenberger, K. Burgstaller, J. Mörtl, in *Proc. of the 30th ISSTech*, Iron and Steel Society, Indianapolis, IN, April **2003**.
- [109] K. Mukai, *ISIJ Int.* **1992**, 32, 19.
- [110] C. Wang, N. Verma, Y. Kwon, W. Tiekink, N. Kikuchi, S. Sridhar, *ISIJ Int.* **2011**, 51, 375.
- [111] I.-H. Jung, G. Eriksson, P. Wu, A. Pelton, *ISIJ Int.* **2009**, 49, 1290.
- [112] Y.-B. Kang, J.-H. Lee, *ISIJ Int.* **2017**, 57, 1665.
- [113] X. Deng, C. Ji, S. Guan, L. Wang, J. Xu, Z. Tian, Y. Cui, *Ironmaking Steelmaking* **2019**, 46, 522.
- [114] W. C. Doo, D. Y. Kim, S. C. Kang, K. W. Yi, *ISIJ Int.* **2007**, 47, 1070.
- [115] Y.-J. Park, W.-Y. Kim, Y.-B. Kang, *J. Eur. Ceram. Soc.* **2021**, 41, 7362.
- [116] C. Wang, N. T. Nuhfer, S. Sridhar, *Metall. Mater. Trans. B* **2010**, 41, 1084.
- [117] Y. Wang, A. Karasev, J. H. Park, P. G. Jönsson, *Metall. Mater. Trans. B* **2021**, 52, 2892.
- [118] I. Korobeinikov, D. Chebykin, S. Seetharaman, O. Volkova, *Int. J. Thermophys.* **2020**, 41, 56.
- [119] M. Burty, P. Dunand, J. P. Ritt, H. Soulard, A. Blanchard, G. Jeanne, F. Penet, R. Pluquet, I. Poissonet, in *Proc. of the 56th ISS Ironmaking Conf.*, Chicago, IL, April **1997**, p. 647.
- [120] L. Zhang, L. Cheng, Y. Ren, J. Zhang, *Ceram. Int.* **2020**, 46, 15674.
- [121] K. Nogi, K. Ogino, *Can. Metall. Q.* **1983**, 22, 19.
- [122] M. Humenik, W. D. Kingery, *J. Am. Ceram. Soc.* **1954**, 37, 18.
- [123] P. Shen, L. Zhang, J. Fu, H. Zhou, Y. Wang, L. Cheng, *Ceram. Int.* **2019**, 45, 11287.
- [124] B. V. Tsarevskii, S. I. Popel, *Chern. Metall.* **1960**, 8, 15.
- [125] P. Kozakevitch, M. Olette, *Rev. Met. Paris* **1971**, 68, 635.
- [126] J. Jeon, S. Kim, M. Kim, H. Park, *Metall. Mater. Trans. B* **2019**, 50, 2251.
- [127] A. Staronka, W. Gotas, *Archiv Eisenhüttenwesen* **1979**, 50, 237.
- [128] B. J. Monaghan, M. W. Chapman, S. A. Nightingale, *ISIJ Int.* **2010**, 50, 1707.
- [129] H. S. Park, Y. Kim, S. Kim, T. Yoon, Y. Kim, Y. Chung, *Ceram. Int.* **2018**, 44, 17585.
- [130] Z. Deng, M. Zhu, Y. Zhou, D. Sichen, *Metall. Mater. Trans. B* **2016**, 47, 2015.
- [131] C. Bernhard, G. Xia, A. Karasangabo, M. Egger, A. Pissenberger, in *Proc. of the 7th ECCS*, Düsseldorf, June **2011**.
- [132] Z. Deng, L. Chen, G. Song, M. Zhu, *Metall. Mater. Trans. B* **2020**, 51, 173.
- [133] P. Kaushik, H. Pielet, H. Yin, *Ironmaking Steelmaking* **2009**, 36, 572.
- [134] E. Zinngrebe, S. van der Laan, A. Westendrop, H. Visser, J. Small, C. van Hoek, in *Proc. of the 9th Clean Steel Conf.*, Budapest, September **2015**.
- [135] J.-H. Lee, M.-H. Kang, S.-K. Kim, J. Kim, M.-S. Kim, Y.-B. Kang, *ISIJ Int.* **2019**, 59, 749.
- [136] Y. Gao, K. Sorimachi, *ISIJ Int.* **1993**, 33, 291.
- [137] H. Zheng, W. Chen, Y. Hu, in *Proc. of the AISTech 2004*, AIST—Association for Iron & Steel Technology, Nashville, TN, September **2004**, p. 937.
- [138] M. Alavanja, R. T. Gass, R. W. Kittridge, H. T. Tsai, in *Proc. of the 78th Steelmaking Conf.*, Iron and Steel Society, Nashville, TN, April **1995**, p. 415.

- [139] R. Dekkers, B. Blanpain, P. Wollants, F. Haers, B. Gommers, C. Verbruggen, *Steel Res.* **2003**, *74*, 351.
- [140] B. Harcsik, P. Tardy, G. Karoly, R. Jozsa, in *Proc. of the 8th Int. Conf. on Clean Steel*, Budapest May **2012**.
- [141] B. Harcsik, G. Karoly, *Steel Res. Int.* **2013**, *84*, 129.
- [142] H. H. Visser, W. Tiekink, M. Koolwijk, R. Kooter, F. Mensonides, J. Brockhoff, in *Proc. of the 7th Int. Conf. on Clean Steel*, Budapest, June **2007**.
- [143] A. R. McKague, R. Engel, M. A. Suer, D. J. Wolf, M. D. Garbowski, L. E. Reed, in *Proc. 56th Electric Furnace Conf.*, Iron and Steel Society, New Orleans, LA, November **1998**, p. 553.
- [144] S. Liu, S. Niu, M. Liang, C. Li, X. Wang, in *Proc. of the AISTech 2007*, AIST—Association for Iron & Steel Technology, Indianapolis, IN, May **2007**, p. 1.
- [145] S. Liu, X. Wang, X. Zuo, Y. Wang, L. Zhang, S. Niu, M. Liang, C. Li, *Rev. Met. Paris* **2008**, *105*, 72.
- [146] F. Fuhr, C. E. Cicutti, G. Walter, G. Torga, in *Proc. of the 30th ISSTech Conf.*, Iron and Steel Society, Indianapolis, IN, April **2003**, p. 53.
- [147] S. K. Michelic, P. Dorrer, G. Kloesch, J. Reiter, A. Paul, C. Bernhard, in *Proc. of the AISTech2017*, AIST—Association for Iron & Steel Technology, Nashville, IN, May **2017**, p. 1555.
- [148] A. Hamoen, W. Tiekink, in *Proc. of the 81st Steelmaking Conf.*, Toronto, CA, March **1998**, p. 229.
- [149] L. Zheng, A. Malfiet, P. Wollants, B. Blanpain, M. Guo, in *Proc. of the 6th Int. Congress on the Science and Technology of Steelmaking*, Beijing, CN, May **2015**, p. 731.
- [150] L. Zheng, A. Malfiet, P. Wollants, B. Blanpain, M. Guo, *ISIJ Int.* **2016**, *56*, 926.
- [151] E. Zingrebe, C. van Hoek, H. Visser, A. Westendorp, I.-H. Jung, *ISIJ Int.* **2012**, *52*, 52.
- [152] M.-K. Sun, I.-H. Jung, H.-G. LEE, *Met. Mater. Int.* **2008**, *14*, 791.
- [153] T. Dubberstein, A. Jahn, M. Lange, H.-P. Heller, P. R. Scheller, *Steel Res. Int.* **2014**, *85*, 1220.
- [154] B. J. Keene, *Slag Atlas 2nd Edition*, Verlag Stahleisen GmbH, Düsseldorf **1995**.
- [155] H. Shibata, X. Jiang, M. Valdez, A. W. Cramb, *Metall. Mater. Trans. B* **2004**, *35B*, 179.
- [156] T. Emi, H. Shibata, H. Yin, in *Proc. of the Belton Memorial Symp.*, Sydney, January **2000**, p. 195.
- [157] S. Kimura, K. Nakajima, S. Mizoguchi, H. Hasegawa, *Metall. Mater. Trans. A* **2002**, *33A*, 427.
- [158] S. Kimura, Y. Nabeshima, K. Nakajima, S. Mizoguchi, *Metall. Mater. Trans. B* **2000**, *31B*, 1013.
- [159] H. Luo, *Scand. J. Metal.* **2001**, *30*, 212.
- [160] K. Nakajima, S. Mizoguchi, *Metall. Mater. Trans. B* **2001**, *32B*, 629.
- [161] B. Coletti, S. Vantilt, B. Blanpain, S. Sridhar, *Metall. Mater. Trans. B* **2003**, *34B*, 533.
- [162] W. Mu, N. Dogan, K. S. Coley, *Metall. Mater. Trans. B* **2017**, *48*, 2379.
- [163] Y. Kang, B. Sahebkar, P. R. Scheller, K. Morita, D. Sichen, *Metall. Mater. Trans. B* **2011**, *42B*, 522.
- [164] S. K. Michelic, U. Dieguez-Salgado, C. Bernhard, in *Proc. of the Int. Symp. Liquid Metal Processing and Casting*, Leoben, September **2015**, p. 143.
- [165] N. Kasai, M. Kawasaki, Y. Hayashi, H. Kawai, *Taikabutsu Overseas* **1991**, *11*, 22.
- [166] H. Shikano, T. Harada, S. Iitiska, S.-I. Kataoka, *Taikabutsu Overseas* **1991**, *11*, 10.
- [167] V. Brabie, *ISIJ Int. suppl.* **1996**, *36*, 109.
- [168] R. Tsujino, A. Tanaka, A. Imamura, D. Takahashi, S. Mizoguchi, *ISIJ Int.* **1994**, *34*, 853.
- [169] F. Ohno, T. Muroi, K. Oguri, *J. Tech. Assoc. Refract.* **2002**, *22*, 63.
- [170] M. Nakamura, T. Yamamura, O. Nomura, R. Nakamura, E. Iida, *Taikabutsu Overseas* **1997**, *17*, 34.
- [171] K. Sasai, Y. Mizukami, *ISIJ Int.* **1994**, *34*, 802.
- [172] N. Yamauchi, K. Yamaguchi, S. Takahashi, in *Proc. of the 3rd Int. Conf. on Science and Technology of Steelmaking*, Charlotte, NC, May **2005**, p. 149.
- [173] O. J. Rajtora, D. C. Van Aken, J. D. Smith, in *Proc. of the Inter. Symp. on Advances in Refractories for the Metallurgical Industries* Montreal, August **2004**, p. 855.
- [174] J. Poirier, D. Verrelle, B. Thillou, G. Provost, C. Taffin, P. Tssot, in *Proc. of the Unitecr '91*, Aachen, September **1991**, p. 226.
- [175] F. G. Wilson, M. J. Heesom, A. Nicholson, A. W. D. Hills, *Ironmaking Steelmaking*, **1987**, *187*, 296.
- [176] E. Kawecka-Cebula, Z. Kalicka, J. Wypartowicz, *Arch. of Metall. Mater.* **2006**, *51*, 261.
- [177] C. Xuan, A. V. Karasev, P. G. Jönsson, K. Nakajima, *Steel Res. Int.* **2017**, *88*, 1600090.
- [178] P. M. Benson, Q. K. Robinson, H. K. Park, in *Proc. of the 76th Steelmaking Conf.*, Iron and Steel Society, Dallas, TX, March **1993**, p. 533.
- [179] T. Aoki, T. Nakamura, H. Ozeki, A. Elksnitis, in *Proc. of the 74th Steelmaking Conf. Proc.*, Iron and Steel Society, Washington, DC **1991**, p. 357.
- [180] N. Tsujino, Y. Kurashina, K. Yanagawa, *Taikabutsu Overseas* **1995**, *15*, 43.
- [181] T. Nakamura, T. Aoki, H. Okumura, Y. Kondo, *Taikabutsu Overseas* **1991**, *11*, 38.
- [182] K. Oguri, M. Ando, T. Muroi, T. Aoki, H. Okamura, in *Proc. of the Unitecr '93*, Sao Paulo, October **1993**.
- [183] R. B. Tuttle, J. D. Smith, K. D. Peaslee, *Metall. Mater. Trans. B* **2007**, *38B*, 101.
- [184] M. Nakamura, T. Yamamura, O. Nomura, R. Nakamura, E. Iida, *Taikabutsu Overseas* **1996**, *17*, 34.
- [185] D. B. Hoggard, H. K. Park (*Vesuvius Crucible Company*) utility patent EP 0309225 A2, **1989**.
- [186] E. Lührsen, A. Ott, W. Parbel, J. Piret, R. Ruddleston, B. Short, in *Proc. of the 1st ECCC*, Florence, September **1991**.
- [187] B. Prasad, J. K. Sahu, J. N. Tiwari, S. K. Chaudhuri, in *Proc. of the 5th ECCC*, Nice, June **2005**.
- [188] J. Svensson, PhD thesis, *KTH Royal Institute of Technology*, **2017**.
- [189] J. Poirier, *Metall. Res. Technol.* **2015**, *112*, 410.



Susanne Michelic has been an associate Professor for Steelmaking at the Montanuniversität Leoben since 2018 and the head of the Christian Doppler Laboratory for Inclusion Metallurgy in Advanced Steelmaking since 2021. She received her Ph.D. in metallurgy at the Montanuniversität in 2011. Her research focuses on steel cleanliness, especially on inclusion characterization and inclusion behavior in the system-steel-slag-refractory.



Christian Bernhard is an associate Professor for steelmaking and casting at the Montanuniversität Leoben. He led the Christian Doppler Laboratory for Metallurgical Fundamentals of Continuous Casting Processes from 2002 to 2009. His current research focuses on continuous casting and secondary metallurgy, especially the defect formation in the casting process and computational thermodynamics.